

## CORNELL STATUS REPORT\*

H. Padamsee, S. Belomestnykh, R. Geng, J. Knobloch, V. Shemelin, G. Werner, Z. Yang  
Laboratory of Nuclear Studies, Cornell University, Ithaca NY, USA

### Abstract

Cornell continues activities in many areas: systems development and operation for CESR, supporting technology transfer of CESR SRF systems to storage ring light sources around the world, collaboration with the world-wide TESLA project, collaboration with Muon Collider/Neutrino Factory projects, developing an Energy Recovery Linac (ERL) based light source in collaboration with JLAB, and basic R&D in the areas of high field Q-slope, field emission, voltage breakdown and waveguide multipacting. We also played a major role in the convincing the SNS to see the benefits of the superconducting option.

### 1 CESR SRF

Over the last three years the primary effort of the SRF program was the development, construction, installation and operation of four single-cell superconducting RF systems to raise the luminosity of CESR. Each single-cell superconducting cavity replaced a high impedance, 5-cell copper cavity. CESR has been running smoothly with SRF systems since October 1997, each operating at a gradient of 6.5 MV/m, and each providing beam power of 280 kW. In machine studies we showed that the best cavity can operate at 8 MV/m and the highest beam power delivered is 290 kW. After installation of SRF systems CESR beam current rose steadily from 350 mA to 750 mA. We also prepared a fifth SRF system as a spare. [1]

To operate the new systems, two 600-watt refrigerators and cryogen distribution system were installed and commissioned. A program is underway to acquire two new industrially fabricated SRF cavity systems in order to shorten CESR bunch length with higher voltage.

### 2 LIGHT SOURCES

We are transferring CESR SRF technology to ACCEL company in Germany who will build turn-key CESR SRF systems for storage rings. Taiwan Light Source will upgrade their machine with such a system [2]. We assisted the Canadian Light Source and the DIAMOND light source (Daresbury/Rutherford collaboration). Both new facilities have selected CESR superconducting cavities [3].

Synchrotron radiation (SR) has proven to be immensely important for the physical, biological, and engineering sciences. The demand for SR continues to grow, with new uses opening all the time. Currently, all major SR sources are based on storage rings. We propose a synchrotron source based on closed-loop energy

recovery with superconducting linacs [4]. Such a machine offers significant advantages to storage ring sources, both in terms of the x-ray beams and cost-effectiveness. The feasibility of operating an ERL has recently been demonstrated with a highly successful free electron laser (FEL) at Jefferson Laboratory [5]. Our long-term goal is to build a high energy (~ 5- 7 GeV) SR source at Cornell, both as a development laboratory for ERL technology and as a unique SR resource. Before committing to specific designs of a large and expensive machine, it is essential to explore key machine issues on a high current prototype machine.

The characteristics of x-ray produced by a SR source are limited by the qualities of electron beams used to produce the SR. Specifically, it is desired to have

- (1) Low electron beam emittance in order increase the brilliance and coherence of SR;
- (2) Very short electron bunches to enable fast time-resolved experiments;
- (3) Round, small cross-sectional area bunches with sharp edges to enable micro-beams, that improve through-put on the x-ray optics and that pass through long narrow-gap undulators;
- (4) A SR output which does not decay over time.

In a storage ring, the important beam characteristics are a function of the entire ring. These characteristics are near in-principle limits in existing 3<sup>rd</sup> generation rings, such as ESRF and APS. Although some improvement is possible, storage ring technology is at the point of diminishing returns and improvements will come at enormous cost.

ERL takes an entirely different approach. Electrons are not stored, so constraints of beam equilibrium never become a limit. Photoinjectors can achieve bunches with emittances, shapes, lengths, etc. which are superior in many important ways to bunches in storage rings. ERL bunches are accelerated to high energy via a superconducting linac (SC linac), which preserves the salient beam characteristics. Superior high energy bunches pass through undulators to produce SR beams with unprecedented characteristics. The ERL has the enormous advantage that beam quality is limited by the photoinjector, rather than the machine as a whole.

A difficulty with any SR source is that the required beam currents carry enormous power, e.g., a 5 GeV, 100 mA electron beam carries 500 MW of power. Therefore, it is economically unfeasible to simply dump the electrons once they have been accelerated. In a storage

ring, the power costs are kept down by reusing the energetic electrons many times.

ERLs resolve the power dilemma by reusing the beam energy. As schematized in Fig. 1, after producing SR, the electrons in an ERL re-enter the SC linac, but 180° out of accelerating phase. The bunches then decelerate and yield their energy back to the electromagnetic field in the linac. When bunches emerge from the linac with the low injector energy (minus SR losses), a weak bending magnet deflects them into a beam dump. The energy recovered by the linac accelerates new electrons. An ERL differs from a storage ring in that energy recirculates, instead of the beam.

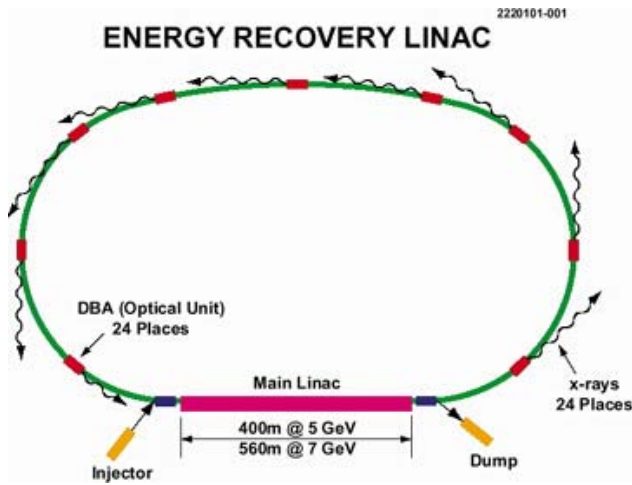


Figure.1: Layout for a future ERL

As a necessary prelude to a proposal to build a large, high-energy Phase II ERL, Cornell proposes to build a small, 100 MeV Phase I ERL (Fig. 2) to resolve outstanding machine physics issues,

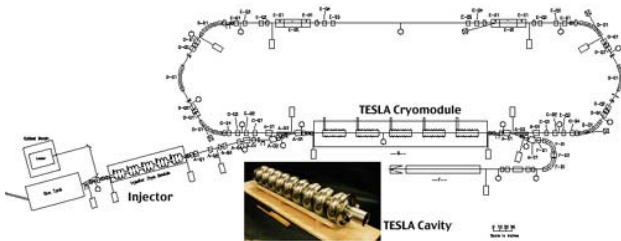


Figure. 2: Layout for a prototype ERL

### 3 NEUTRINO FACTORY AND MUON COLLIDER COLLABORATION

Over the last year, LNS assisted the Muon Collaboration to choose parameters for the RF and acceleration systems for the Neutrino Factory Feasibility Studies I and II, conducted by Fermilab, LBNL and BNL [6]. New cavity geometries were developed for 200 MHz cavities to give low surface fields that will accompany the 15 - 17 MV/m gradient needed for rapid muon

acceleration. A collaboration has been set up with CERN to produce a one-cell Nb/Cu cavity at 200 MHz. To date, the half-cells have been spun and preparation underway for welding. To test the large cavity, Cornell is upgrading its preparation and test facilities. A test pit 2.5 m diameter by 5 meter deep (Fig. 3) has been excavated to accommodate the test dewar, also acquired. Radiation shielding construction is complete. A 200 MHz low power (2 kW) RF test system is complete. Installation is nearly complete for a 1100 sq ft clean room.



Figure 3: Test pits for various size cavities.

At 200 MHz, structure costs will be substantial. Multicell cavities are usually fabricated in parts that have to be machined, cleaned and electron beam welded. This is an expensive, labor intensive process. We are collaborating with INFN in Italy to spin monolithic copper cells out of a single tube. INFN has experience at 1300 MHz. As a first step they will spin a single cell 500 MHz cavity. Dies have been made and the first spinning carried out from a copper pipe. In a future stage, the procedure will be extended to 200 MHz and two-cell cavities.



Figure 4: INFN 500 MHz cavity by spinning from tube.

### 4 BASIC R&D FIELD EMISSION

Experience with operating cavity systems at CESR, JLAB, LEP-II and TTF show the need for an in-situ technique to limit field emission from dirt that may

accidentally get into accelerator cavities during final assembly, accelerator installation, or long-term operation. If fields are pushed to higher values even for short times, emission eventually leads to voltage breakdown with mostly a beneficial effect, known as conditioning. After a voltage breakdown event, it is usually possible to raise the electric field until field emission grows intense once again at another emitter on the cavity surface. Gradient gains of factors of 3 are common[7].

We have developed special vehicles to study breakdown in both RF and DC fields [8]. Through these devices we have advanced our basic understanding of voltage breakdown. Studies show that voltage breakdown in niobium cavities bears strong commonalities with DC voltage breakdown on room temperature cathodes[9].

Since microparticle are common field emitters, we are studying the physics of voltage breakdown using microparticles of carbon, nickel, indium, vanadium and other elements as intentional emitters that trigger breakdown. We are also studying the influence of adsorbed gas. Voltage breakdown sites are analysed using SEM/EDX and Auger analysis systems.

A digital video camera captures cathode light spots Fig. 5) during DC breakdown of electrodes. Fig. 6 shows a scanning electron micrograph (SEM) of a vanadium particle responsible for breakdown on a niobium cathode. At the breakdown site we find a central molten crater with a residue of the original V particle as a thin coating. Even though the original particle was several microns in diameter, the breakdown event was so violent that there is no trace of V in the crater to the sensitivity of the energy dispersive x-ray analysis system (EDX). But a scanning Auger analysis clearly reveals a thin coating of vanadium over the entire crater (Fig. 6). As before, we find micron size craters surrounded by starbursts, regions of low secondary emission coefficient that show up in the SEM. Scanning Auger maps show that the starburst feature is poor in carbon and fluorine indicating that the starburst is a cleaner region, most likely because of ion bombardment by gases during the breakdown. When extraneous particles are present in the region of the starburst they either melt or completely evaporate, also presumably due to the intense ion bombardment.

We are extending breakdown studies to copper electrodes since this is a serious problem for high gradient copper cavities. Fig. 7 shows a region of breakdown initiated by a vanadium particle intentionally placed on an electropolished copper cathode. Once again there is a principal crater with a thin vanadium coating revealed by Auger. The crater is surrounded by a starburst, poor in carbon as revealed by Auger. But the starburst is scraggly, unlike those on niobium. Another discovery is that many craters are present all over the starburst region on the copper cathode as compared to just a few craters on a niobium cathode. Differences between copper and niobium breakdown provide valuable clues to the nature and evolution of voltage breakdown.

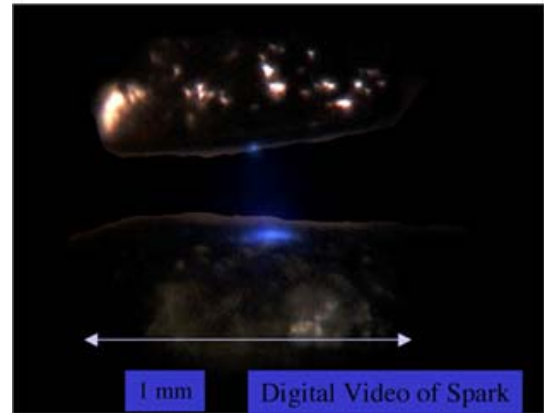


Figure 5: Spark on a cathode (upper electrode)

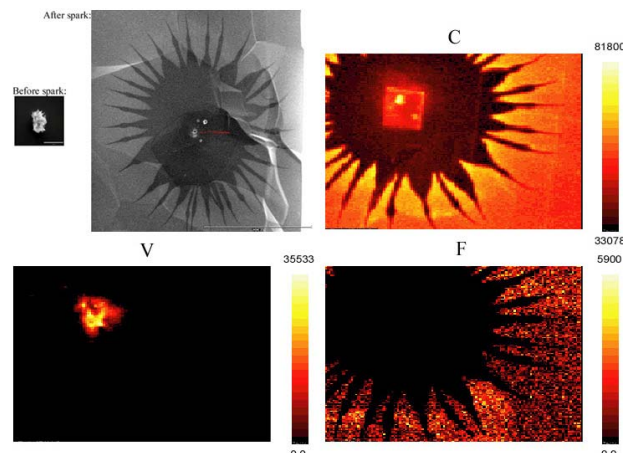


Figure 6: SEM and Auger images of sparked cathode caused by a vanadium particle on niobium.

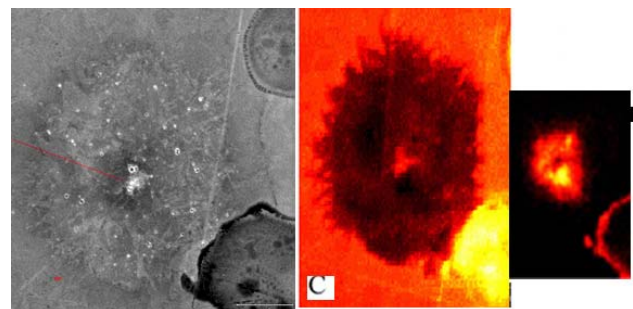


Figure 7: SEM and Auger Images of a spark caused by a Vanadium particle on a copper cathode.

## 5 HIGH FIELD Q-SLOPE

In chemically etched cavities that show little or no field emission, there persists a steady decline in  $Q_0$  above 20 MV/m (the so-called high-field Q-slope), followed by a quench between 20 and 30 MV/m (Fig. 8). Absence of x-rays corroborates the absence of field emission. Temperature maps with our 760 fixed thermometer system reveal that power dissipation occurs over large areas in the high magnetic field regions of the cavity. Yet

the losses are not uniform (Fig. 9). Baking also has a slight beneficial effect on the Q-slope of chemically etched cavities, but no significant effect on the quench field. Fig. 10 shows the effect of baking on some of the hot patches, and Fig. 11 shows the effect of re-oxidation followed by a second bake. Even though the baking effect on the overall Q-slope does not appear very dramatic, the temperature map shows a pronounced disappearance of many patches. More interesting is the discovery that the exponent of the Q-slope is significantly different after baking. Figures 12 and 13 compare the exponents before and after baking. There is a big drop for most exponent values, from 10-15 down to 5-10. Yet there remain stubborn patches of Q-slopes with exponents of 10 – 15. The quench field and location did not change on baking or rebaking.

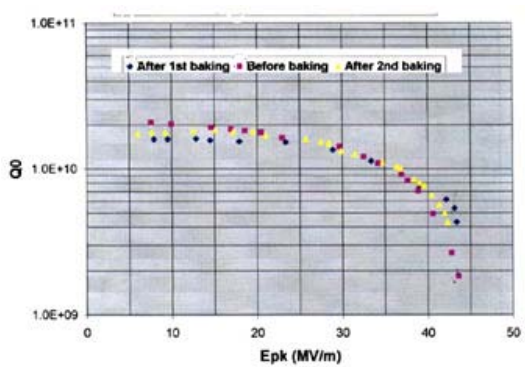


Figure 8: High field Q-slope on an etched 1300 MHz single cell cavity.

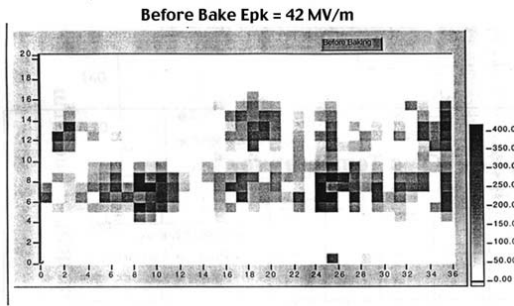


Figure 9: Temperature map showing regions responsible for Q-slope.

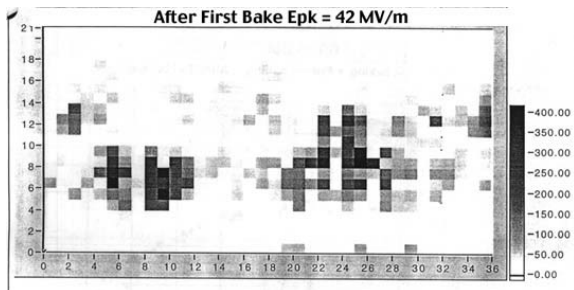


Figure 10: Temperature map after bake.

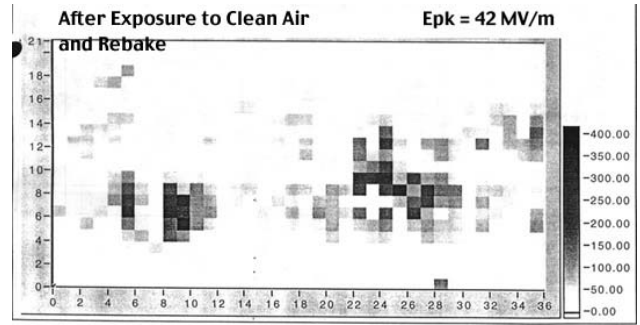


Figure 11: Temperature map after re-oxidation and bake.

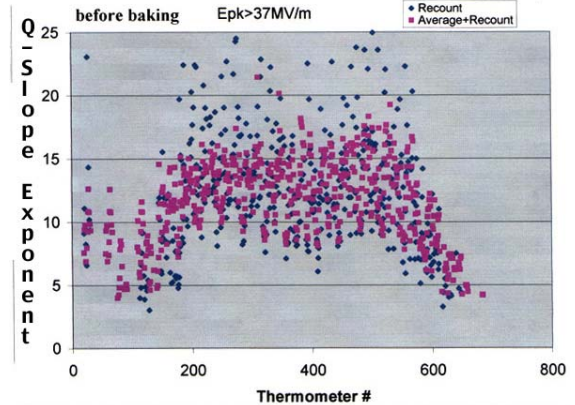


Figure 12: Range of Q-slope exponents before bake.

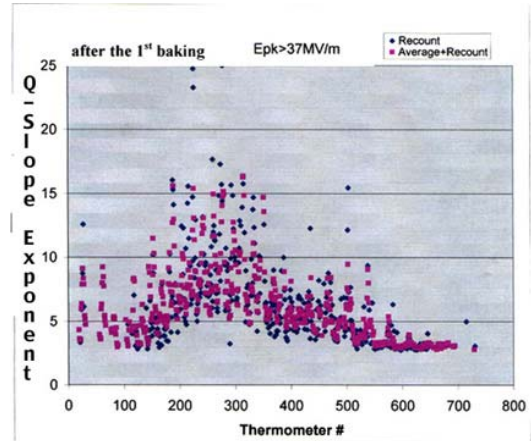


Figure 13: Range of Q-slope exponents after bake.

## 6 BASIC R&D WAVEGUIDE MULTIPACTING

Calculations have been carried out to characterize multipacting in reduced height waveguides under travelling wave, reflected and mixed wave conditions to understand and enhance performance of the waveguide input coupler (Fig. 14) for CESR cavities[10]. MAFIA and multipactor simulations were carried out to simulate the effect of a groove along the high electric field region to stop multipacting in the waveguide. Results (Fig. 15) are encouraging enough to warrant a high power test. On the other hand, wedged waveguide geometries with taper angles as high as 13.5 degrees did not suppress multipacting.

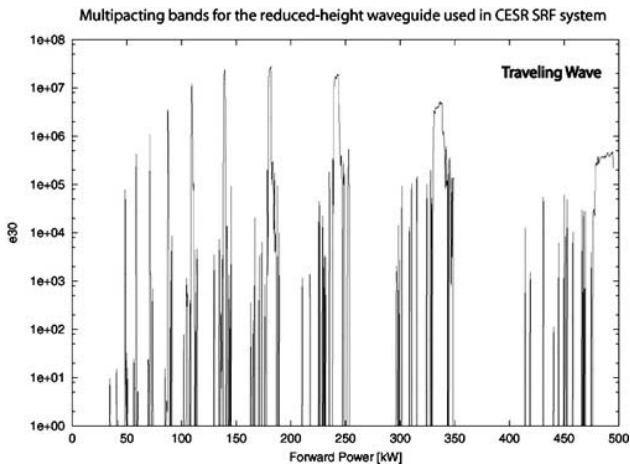


Figure 14: Multipacting levels for reduced height waveguide in CESR 500 MHz cavity input coupler.

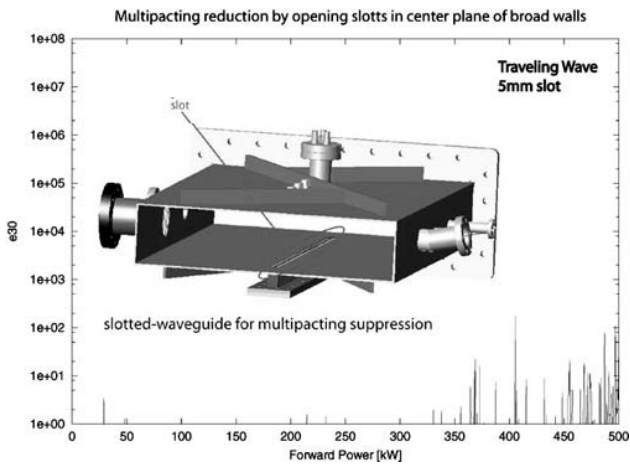


Figure 15: Suppression of multipacting with a groove.

## 7 REFERENCES

- [1] S. Belomestnykh, Proceedings of the 1999 Particle Accelerator Conference, NY, E. A. Luccio and W. Mackay, p. 272 (1999).
- [2] M. Pekeler et al, Proceedings of the 2001 Particle Accelerator Conference, Chicago, paper MPPH 166 (2001).
- [3] M. de Jong, Proceedings of the 2001 Particle Accelerator Conference, Chicago, Paper TOPA002 (2001).
- [4] ERL study at <http://erl.chess.cornell.edu>.
- [5] G. Neil et al, Nucl. Inst. and Meth. in Phys. Res. B144, p. 40 (1998).
- [6] N. Holtkamp et al, FERMILAB-PUB-00-108-E (2000) & S. Ozaki et al, "Feasibility Study II of a Muon-Based Neutrino Source," Ed., J. Gallardo (2001).
- [7] C. Crawford et al., Particle Accelerators, 49, 1 (1995).
- [8] H. Padamsee in High Energy Density Microwaves, AIP Conference Proceedings 474, Ed. R. Phillips, p. 212 (1998).
- [9] G. Werner et al, Proceedings of the 2001 Particle Accelerator Conference, Chicago, paper MPPH127 (2001).
- [10] R. Geng et al, Proceedings of the 2001 Particle Accelerator Conference, Chicago, paper MPPH 320 (2001).